JOURNAL OF Applied Polymer SCIENCE

The Effect of Morphology on the Corrosion Inhibition and Mechanical Properties of Hybrid Polymer Coatings

Jaspreet Singh-Beemat, Jude O. Iroh
Material Science and Engineering Program, School of Aerospace Systems, University of Cincinnati, Cincinnati, Ohio 45221-0012
Correspondence to: J. O. Iroh (E-mail: jude.iroh@gmail.com)

ABSTRACT: The durability and mechanical properties of epoxy ester coatings and films has been improved by blending with rigid aromatic polyurea (PU). The interaction of PU and epoxy ester was enhanced by coupling the polymers with polymethylhydrosiloxane. The reactions between various entities are analyzed by Fourier transform infrared spectroscopy and the change in physical and mechanical properties are studied by a dynamic mechanical analyzer. The corrosion resistance of the hybrid coatings was measured by direct current polarization method, direct current polarization (DCP). The addition of polymethylhydrosiloxane enhances the corrosion properties in the hybrid coatings. The surface morphology was analyzed by scanning electron microscopy. The glass transition temperature of the films increases with increasing PU concentration and a wide glass rubber transition range for hybrid coatings was achieved which confirms the higher impact strength of the hybrid coatings and films. © 2012 Wiley Periodicals, Inc. J. Appl. Polym. Sci. 000: 000–000, 2012

KEYWORDS: epoxy ester; polyurea; polymethylhydrosiloxane; corrosion current; storage modulus; glass transition temperature

Received 2 December 2011; accepted 21 April 2012; published online
DOI: 10.1002/app.37961

INTRODUCTION

Polymer blends in the recent past has given new insights into the glass transition, which was otherwise not feasible with pure materials.[1–3] The glass transition temperature (T_g) of a polymer blend is not just necessarily the intermediate of the T_g of the individual polymers because due to the heterogeneous nature of local segments, the motion of one segment is affected by its nearest neighbors in the blend.[4] In a miscible polymer blend the local environment of a monomer of type A is on average be rich in A compared to the bulk composition, and similarly for B because of the direct consequence of chain connectivity. The local segmental motion of the chain exhibit different dependencies on temperature and overall composition and it leads to the broadening of the glass transition temperature, T_g.[5,6] The composition, components molecular weights and architectures also has effect on the local heterogeneities. At a temperature higher than the T_g of lower T_g component, the segmental motions of that component are thermally activated but impeded by steric constraints.[7] The severity of intermolecular constraints can be varied by changing the relative rate of the component dynamics, for example, by changing their T_g, which can be accomplished by variation of their molecular weights that does not involve any changes in chemical structure. The technology of polymer blends has lead to many applications in which the desired properties can be tailored, which otherwise is not feasible by changing the chemistry of the pure components.[8–10]

In this work, the durability of the epoxy ester (EE) paints is improved by utilizing the concept of blending the low T_g EE with a high T_g polyurea (PU) and then incorporating polymethylhydrosiloxane (PMHS) as a coupling agent. The EE combines the chemical resistance of epoxy resin with the processability of unsaturated polyesters.[11,12] The highly reactive epoxide rings limits its use in processing various blends. The epoxy functional group is usually opened by esterification with unsaturated fatty acids to form alkyd modified EEs or by acrylates to form acrylic modified EEs.[13–15] The EEs cure in the same way as their modifiers. The properties of the EEs can be controlled by a number of factors such as the level of unsaturation as well as the chain length of modifiers.[16–18] The longer oil chains results in lower chemical resistance and longer drying times, but it enhances the ability to penetrate and seal a poorly cleaned surface. On the other hand the shorter oil coatings are relatively hard and brittle but have good moisture and chemical resistance.[19] A schematic of EE is shown in Scheme 1 in which the base epoxy resin is reacted with unsaturated fatty acids to generate EE.

The emulsion of EEs in water dries by evaporation of water and then by film formation due to coalesce of the particles. As the

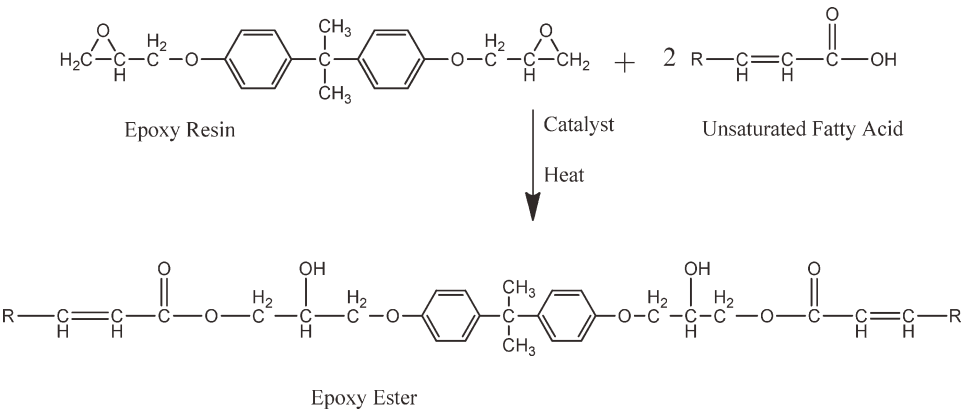

Scheme 1. Chemical structure of EE, where *R* is the modifier group.

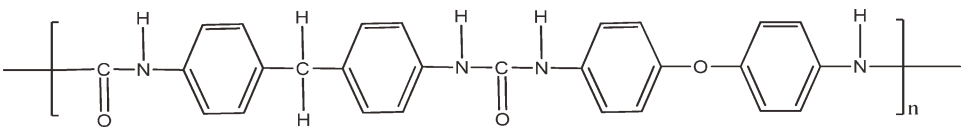

Scheme 2. Chemical structure of PU.

water evaporates the particles come together and diffuse to make a film. The film continues to cure by way of autoxidation depending on the chemistry of the modifier.[20–22]

Autoxidation is the direct reaction of molecular oxygen with organic compounds under mild conditions.[23] The reaction proceeds by a free-radical chain mechanism and can be described in terms of initiation, propagation, and termination.[24–27] Initiation can occur through the action of arbitrary initiating species, directly forming a carbon-centered radical or by thermal homolytic hydroperoxide decomposition. Propagation reactions involve mainly hydroperoxide formation and termination occurs via radical recombination to yield peroxy, ether and carbon–carbon crosslinks. Another termination mechanism is Russel-mechanism, where a tetraoxide intermediate is formed which decomposes to yield nonradical products: an alcohol, ketone and singlet oxygen.[28–30]

EE resins are known for their attractive corrosion inhibiting characteristics, but their use is limited by their inferior chemical and mechanical properties.[31–35] In this study, a novel concept of enhancing the mechanical properties and the durability of EE resins has been introduced. The rigid aromatic PU has been used as a filler due to its compatibity with EE resins. Traditionally used polyurethane/urea is known to have elastomeric properties which are due to the phase separation between hard isocyanate groups and aliphatic soft diol entities.[36–39] The PU used in this study has aromatic entities in its backbone and has little ability to absorb impact (Scheme 2).

The mechanical properties of EE are enhanced due to the increased heterogeneity in the local segments of the blend. The diversified local segmental relaxation time leads to broadening of the T_g of the blend which directly leads to improved impact properties and enhanced durability of the coatings and films of the blend.

To further enhance the interaction of EE and PU, PMHS has been used as a coupling agent. PMHS has been preffered to polydimethylhydrosiloxane (PDMS), due to the additional reactive site of Si—H in PMHS (Scheme 3) as compared to Si—CH_3 in PDMS. PMHS is nontoxic, stable to air and moisture, and inexpensive polymer coproduct of Silicone industry and has been used as a reducing agent for carbonyl compounds to alcohols.[40–43] It is therefore a suitable candidate for low cost environmentally benign corrosion resistant coatings. The other reaction mechanism involves the reaction of the terminal vinyl group in the EE with PMHS by hydrosilylation in the presence of a suitable catalyst and under heat.[44–46] The tendency of PMHS to react with carbonyl groups as well as with double bonds makes it a suitable coupling agent for PU and EE.

EXPERIMENTAL

Materials

The reagents used in this study are as follows: (ODA) 4-4′-Oxydianiline (97% purity), (MDI) 4,4′-Methylenebis(phenyl isocyanate) (98% purity), and *N*-methyl pyrrolidinone (99% purity) were purchased from Sigma-Aldrich Company. EE used for this study was in the form of emulsion in water and provided by Cytec Surface Specialties. PMHS was purchased from Gelest. The Al 2024-T3 Q-panels were purchased from Q-Labs,

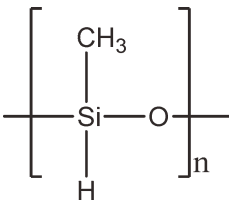

Scheme 3. Chemical structure of PMHS.

Table I. Description of Various Coatings and Films

Composition	Name
Neat epoxy ester	EE
Epoxy ester + x wt% polyurea	EE+PU x wt %
Epoxy ester + PMHS	EE-PMHS
Epoxy ester + PMHS + x wt % polyurea	EE-PMHS-PU x wt %

Cleveland, OH. All the reagents listed above are all analytical grade. Deionized water was also used in this process.

Synthesis of PU

ODA (5.006 g) was added to 100 mL of NMP in a round-three neck flask and stirred for 30 mins using a mechanical stirrer in a nitrogen atmosphere and temperature was maintained at 10°C. MDI (6.2565 g) was added to the solution and stirring was continued for 14 h.

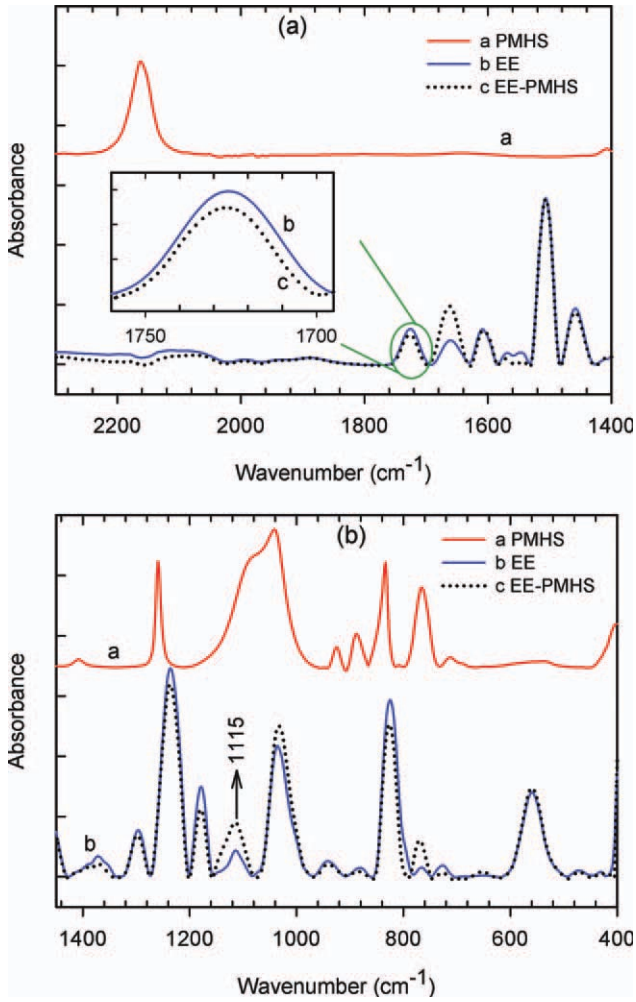

Figure 1. (a) FTIR spectrum of PMHS, EE, and EE-PMHS. (b) FTIR spectrum of PMHS, EE, and EE-PMHS. [Color figure can be viewed in the online issue, which is available at wileyonlinelibrary.com.]

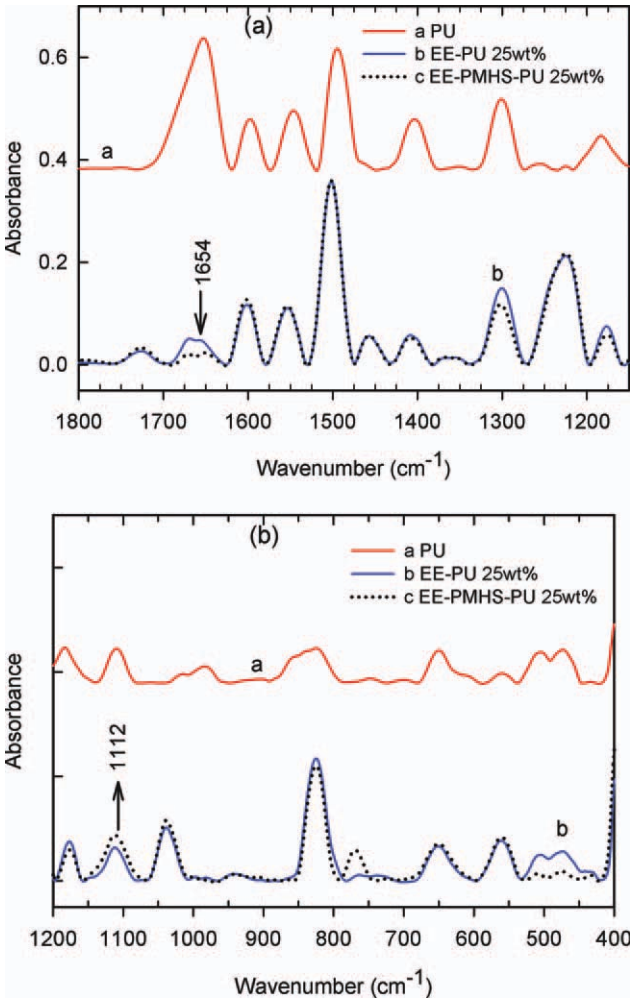

Figure 2. (a) FTIR spectrum of PU, EE-PU 25 wt % and EE-PMHS-PU 25 wt %. (b) FTIR of PU, EE-PU 25 wt % and EE-PMHS-PU 25 wt %. [Color figure can be viewed in the online issue, which is available at wileyonlinelibrary.com.]

Preparation of EE, PMHS, and PU Blend

The EE was mixed with the NMP during high speed mechanical stirring to reduce the particle size of EE emulsion. PMHS was added to the modified EE during stirring. For the hybrid blends, PU was added to NMP and mechanically stirred for 10 mins. Then PMHS was added to the solution (for the blends with PMHS) and after 20 mins, EE was added drop wise with high speed stirring for additional 2 h. Blends were prepared by using varying concentrations of PU. PMHS was maintained constant at 4 wt % for the blends containing PMHS. The description for the coatings and films with various compositions is given in Table I.

Sample Preparation

For corrosion testing, the coatings were prepared by solution drop method onto 1″ × 4″ × 1/8″ Al 2024-T3 coupons. The coatings were cured in a vacuum oven in a stepwise manner, heating initially at 45°C for 4 h, 75°C for 1 h and finally at 100°C for 4 h. The thickness of the coatings was maintained at about 120 μm. Free standing films for dynamic mechanical

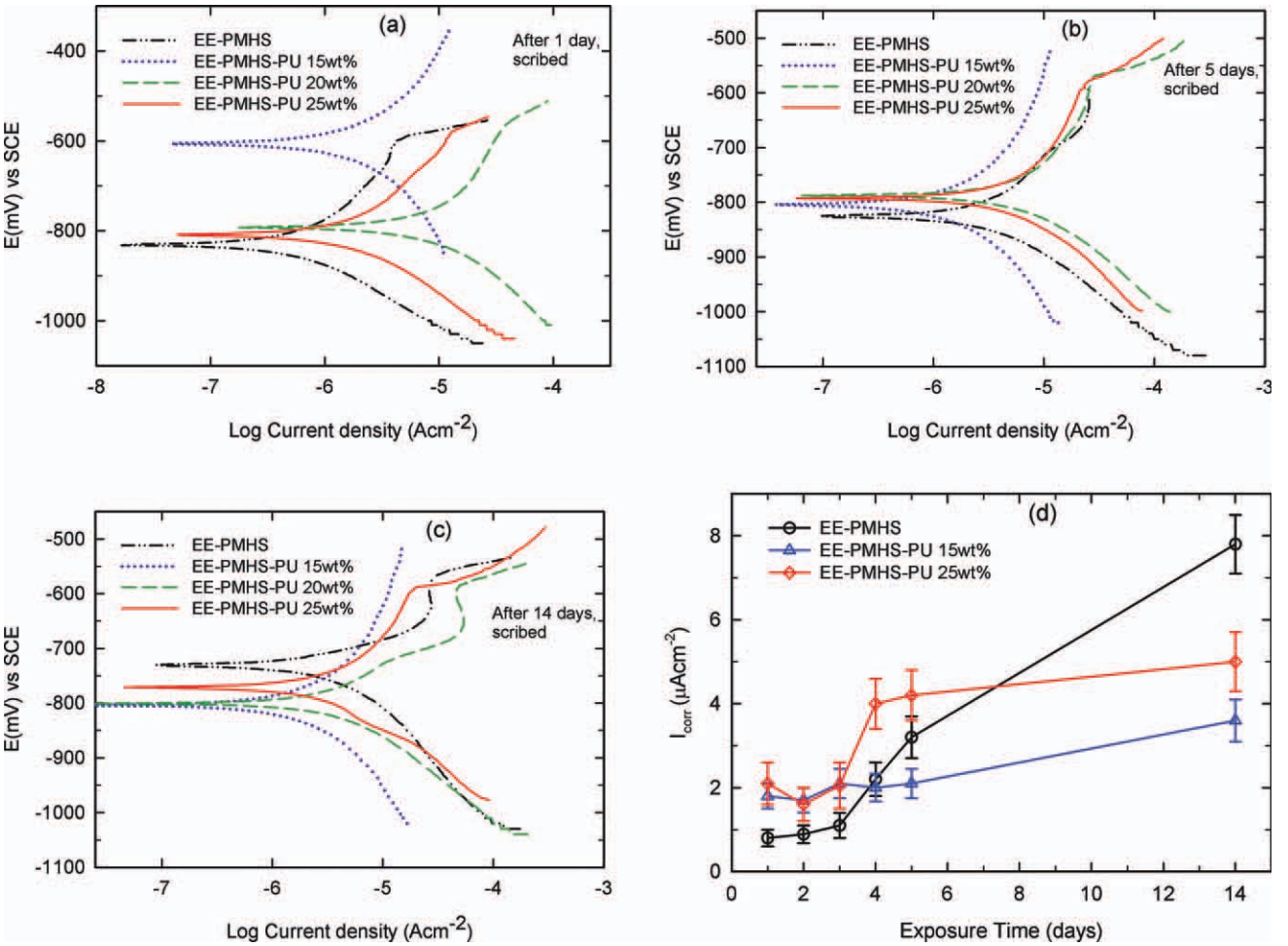

Figure 3. (a) DC polarization curves of EE-PMHS containing various concentrations of PU, after1 day of exposure. (b) DC polarization curves of EE-PMHS containing various concentrations of PU, after 5 days of exposure. (c) DC polarization curves of EE-PMHS containing various concentrations of PU, after 14 days of exposure. (d) I_{corr} as a function of exposure time for EE-PMHS, EE-PMHS-PU 15 wt %, and EE-PMHS-PU 25 wt % coatings up to 14 days of exposure. [Color figure can be viewed in the online issue, which is available at wileyonlinelibrary.com.]

testing were prepared by casting in 1.5″ × 1.5″ × 1/4″ Teflon molds.

Characterization

Nicolet 6700 FTIR instrument equipped with a Smart Orbit ATR accessory with diamond crystal was used to determine the chemical composition of the samples. ATR was performed over a wavenumber range between 4000 cm^{-1} and 400 cm^{-1}.

EG&G 273 A potentiostat equipped with 352 Soft Corr III corrosion software was used to analyze the DC polarization curves. The DC curves were generated by applying a potential in the range from −250 mV to +250 mV from the open circuit potential against a saturated calomel reference electrode, SCE, at a scan rate of 2 mV/s. The coatings were scribed and exposed to a 3.5% sodium chloride solution. DC polarization test was performed on the scribed as well as on the non scribed coated substrate at various intervals of exposure time.

Dynamic mechanical spectroscopy (DMS) was used to study the viscoelastic behavior of the hybrid EE coatings using DMS6000, Seiko Instruments; under tensile loading at a heating rate of 5°C/min and a frequency of 1 Hz. The dynamic mechanical analysis data is plotted in the form of storage modulus against temperature and tan δ against temperature, respectively. The plot of storage modulus against temperature shows the variation of elastic modulus of the coatings with temperature. The glass-rubber transition temperature (T_g) is measured from the temperature corresponding to the midpoint in the drop in the modulus vs. temperature curve or from the temperature corresponding to the peak of the tan δ vs. temperature curve.

Surface morphology was studied using Scanning Electron Microscopy, Hitachi FEG Model. Samples were prepared by solution drop method onto 10 mm × 10 mm Al 2024-T3 panels and then Ag was sputter coated by Polaron SC7640.

RESULTS

ATR Infrared Spectroscopy

The IR plots for PMHS, EE, and EE-PMHS are shown in Figure 1(a, b). PMHS has distinct peaks at 2163 cm^{-1}, 1042 cm^{-1}, and

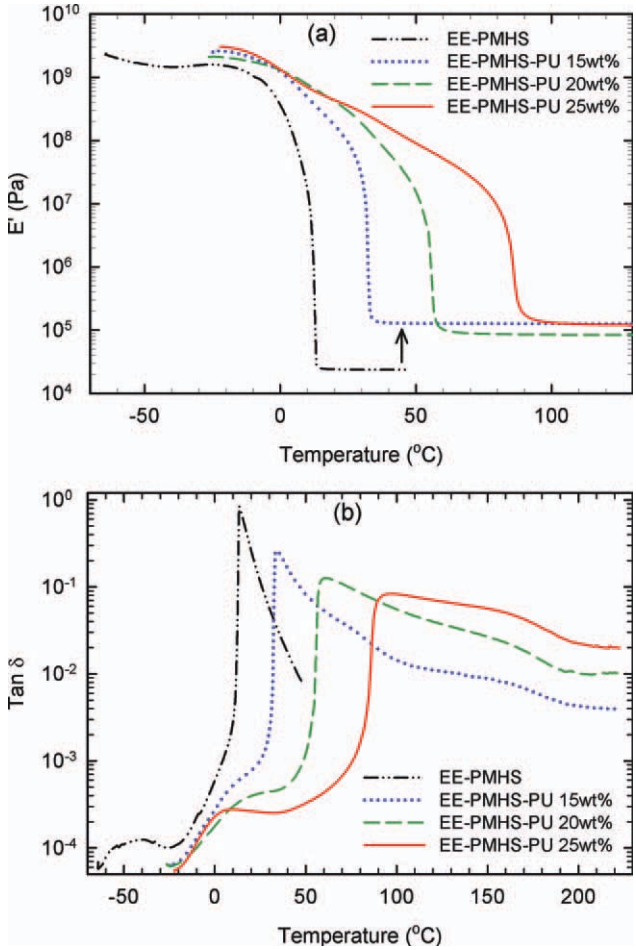

Figure 4. (a) Storage modulus (E') as a function of temperature for EE-PMHS containing various concentrations of PU. (b) Tan δ as a function of temperature of EE-PMHS containing various concentrations of PU. [Color figure can be viewed in the online issue, which is available at wileyonlinelibrary.com.]

1094 cm^{-1} wavenumbers, which belongs to Si—H and Si—O—Si (latter two), respectively. The EE has a carbonyl peak at 1725 cm^{-1} and C—O—C peak at 1115 cm^{-1}. The peak at 1500 cm^{-1} belongs to aromatic structure and is used to normalize the intensity of other groups due to its dormant role in the reactions involved. There is no trace of Si—H peak in EE-PMHS and together with decrease of carbonyl peak and increase of 1115 cm^{-1}, which belongs to C—O—C as well as Si—O—C, confirms the reduction of carbonyl groups of EE with PMHS. Figure 2 shows the IR of PU, EE-PU 25 wt %, and EE-PMHS-PU 25 wt %. The peak at 1654 cm^{-1} belongs to carbonyl of PU and the intensity of this peak in the blend is reduced by the addition of PMHS and together with the increase in 1112 cm^{-1} peak confirms the reaction of carbonyl groups of PU with PMHS.

Direct Current Polarization Test Results

The polarization curves for EE-PMHS coatings with various concentrations of PU are shown in Figure 3(a–c). The corrosion current density, I_{corr} which is directly proportional to the corrosion rate, is calculated from the projection of intersection of slopes of cathodic and anodic arms on the axis showing current density. The I_{corr} for the EE-PMHS coating is lower than the EE-PMHS-PU hybrid coatings after 1 day of exposure [Figure 3(a, d)]. All the coatings except the EE-PMHS-PU 15 wt % hybrid coating has shown passivation behavior in the anodic curves. The passivation behavior is shown by aluminum alloys when exposed to corrosive environment. After 5 days of exposure, the EE-PMHS coating has higher I_{corr} than the EE-PMHS-PU 15 wt % hybrid coating, but less than the other hybrid coatings [Figure 3(b, d)]. The I_{corr} for the EE-PMHS coating becomes comparable to the hybrid coatings of EE-PMHS containing 20 and 25 wt % PU and was remarkably higher than EE-PMHS-PU 15 wt % hybrid coating after 14 days of exposure time [Figure 3(c, d)]. The combination of low I_{corr} and absence of passivation behavior in the anodic region at all exposure times for EE-PMHS-PU 15 wt % hybrid coating proves its better corrosion protection performance.

Dynamic Mechanical Analysis

The dynamic mechanical analysis provides information about the physical as well as mechanical properties of polymers. The T_g is measured from the midpoint of the drop in the log modulus vs. temperature curve or from the temperature corresponding to the peak of the tan δ vs. temperature curve.The presence of PU significantly increases the T_g of EE-PMHS by more than

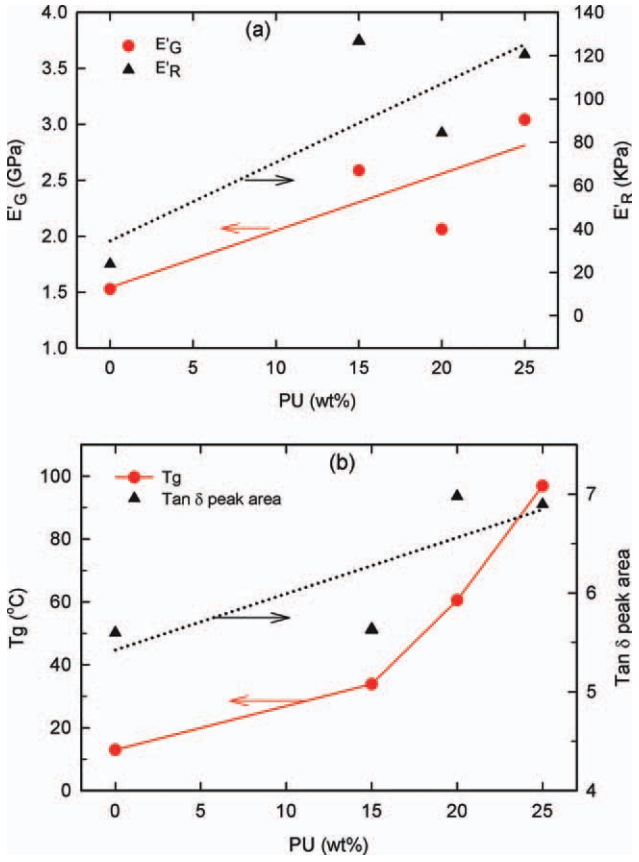

Figure 5. (a) Storage modulus in the glassy state (E'_G) and rubbery state (E'_R) for EE-PMHS containing various concentrations of PU. (b) Tan δ peak area and T_g of EE-PMHS containing varying concentrations of PU. [Color figure can be viewed in the online issue, which is available at wileyonlinelibrary.com.]

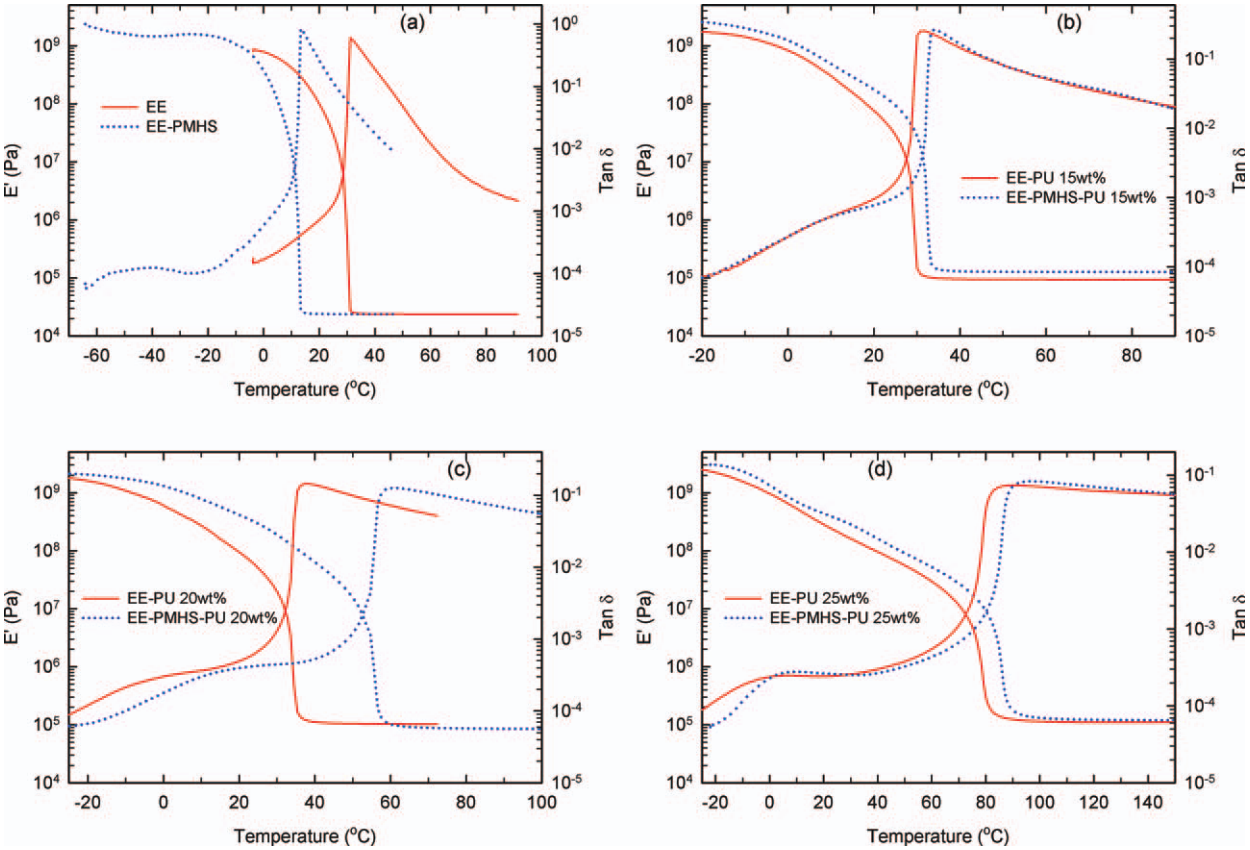

Figure 6. (a) Storage modulus and tan δ as a function of temperature for EE and EE-PMHS. (b) Storage modulus and tan δ as a function of temperature for EE-PU 15 wt % and EE-PMHS-PU 15 wt %. (c) Storage modulus and tan δ as a function of temperature for EE-PU 20 wt % and EE-PMHS-PU 20 wt %. (d) Storage modulus and tan δ as a function of temperature for EE-PU 25 wt % and EE-PMHS-PU 25 wt %. [Color figure can be viewed in the online issue, which is available at wileyonlinelibrary.com.]

80°C with the addition of 25 wt % PU [Figure 4(a, b)]. The storage modulus of all the hybrid films containing PU decreases gradually with temperature in contrast to the sharp fall in EE-PMHS film. The storage modulus, which is manifestation of the rigidity increases in the glassy state ($E_G^{'}$) as well as in the rubbery state ($E_R^{'}$) with the addition of PU [Figure 5(a)]. The $E_R^{'}$ is indicative of the crosslink density and the crosslinking can be physical or chemical.[47] The value of $E_R^{'}$ increases by an order of magnitude with the addition of PU. Figure 5(b) shows the variation of tan δ with temperature for the EE-PMHS containing various concentrations of PU. The α-transition peak temperature which is indicative of the T_g increases with PU content. The enhancement of T_g raises the end use temperature of the hybrid coatings. The area under the α-transition peak which is correlative with the impact energy[48,49] of the films also increases with increasing PU concentration up to 25%.

The storage modulus and tan δ curves of hybrid films containing various concentration of PU with and without PMHS are shown in Figure 6(a–d). For the neat EE, the addition of PMHS reduces the T_g from 33°C to 13°C, but there is no change in $E_R^{'}$. It indicates that the total number of crosslink density remains the same, because modulus in the rubbery region ($E_R^{'}$) is directly proportional to the crosslink density.[47] In the case of hybrid coatings, the T_g of the films increases with the addition of PMHS. The storage modulus in the glassy state ($E_G^{'}$) is higher for all the hybrid films containg PMHS. The increase in T_g with the addition of PMHS is maximum for the films containing 20 wt % PU. The decrease in T_g of EE and increase in T_g of EE-PU films with the addition of PMHS confirms the coupling of EE and PU with PMHS.

Scanning Electron Microscopy

The micrographs of surface morphology of the coatings are shown in Figure 7(a–g). The neat EE shows morphology of uniformly distributed dots. The EE polymers are largely consist of long aliphatic chains of fatty acids. Polar reactive groups are usually grafted at the chain ends of EEs to make them water dispersible.[14] So the small dots consists of collapsed chains of long aliphatic hydrocarbons evenly distributed. PU on the other hand consists of aromatic backbone and having highly polar groups and with the addition of 15 wt % PU in EE, the small dots disappears and no morphological feature can be seen from the SEM images. One of the probable reason is that PU and EE in this study makes an semi-interpenetrating network. The mesh of rigid PU and soft EE chains do not allow the EE chains to collapse, which is also the reason for increased impact strength of the hybrid films and the better durability in the

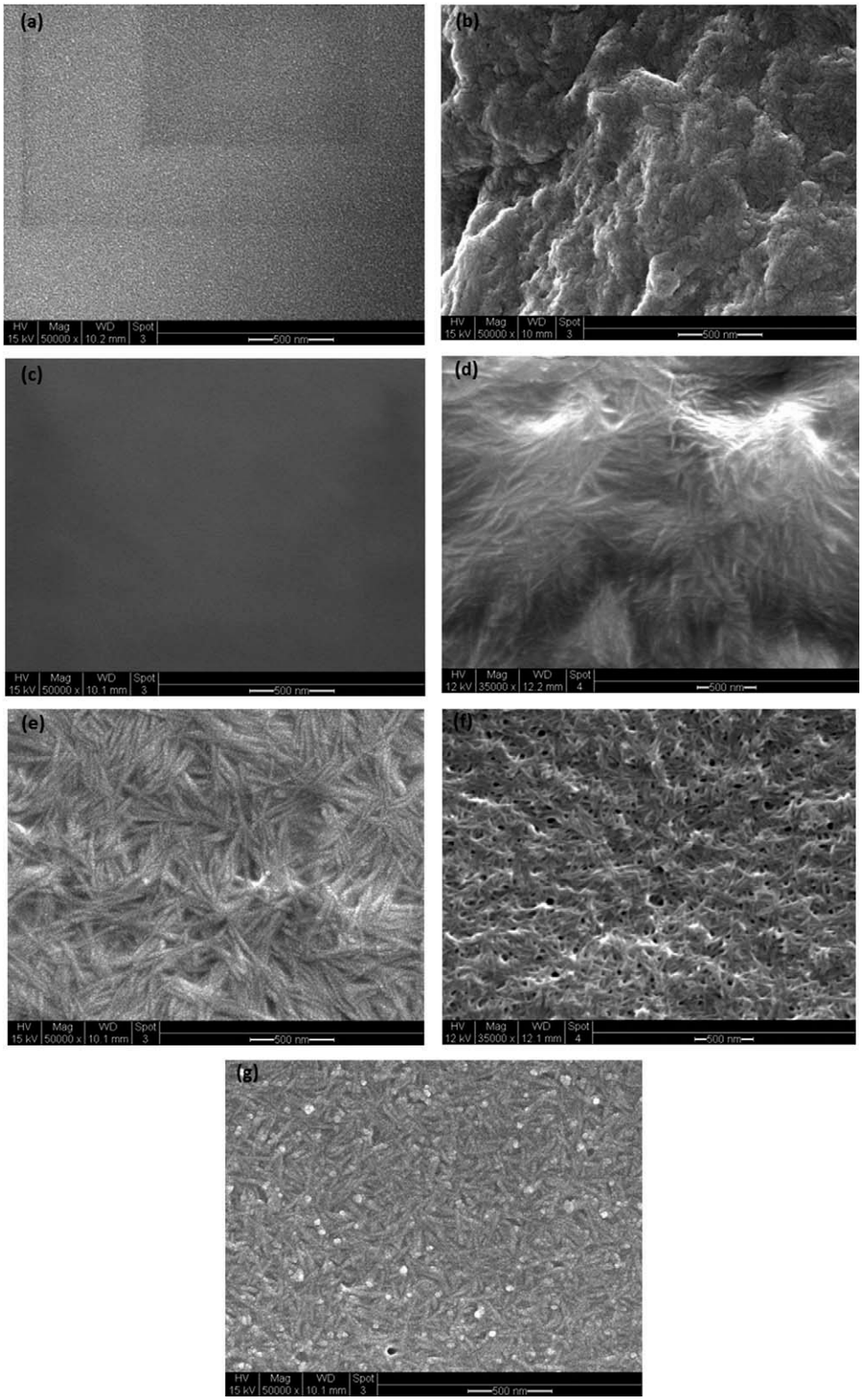

Figure 7. Scanning electron micrographs of (a) EE; (b) PU; (c) EE-PU 15 wt %; (d) EE-PU 20 wt %; (e) EE-PU 25 wt %; (f) EE-PU 30 wt %; (g) EE-PMHS-PU 25 wt %.

corrosion properties. With the increasing concentration of PU, the morphology starts to open up and PU dominates the morphology even at lower concentrations due to its higher rigidity than EE. The same is confirmed from the deteriorating corrosion properties with the increasing PU concentration of more than 25% (not shown here). With the addition of silane, the

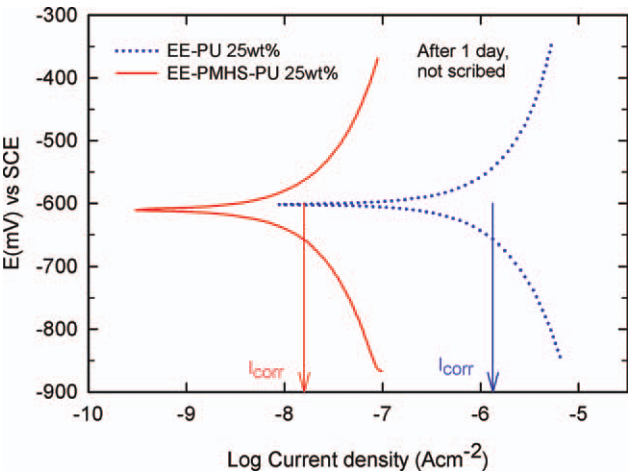

Figure 8. DC polarization curves of EE-PU 25 wt % and EE-PMHS-PU 25 wt % after 1 day of exposure. [Color figure can be viewed in the online issue, which is available at wileyonlinelibrary.com.]

morphology becomes compact as can be seen from comparison of EE-PU 25 wt % with and without PMHS [Figure 7(e, g)]. It confirms the coupling of EE and PU in the presence of PMHS. It leads to superior barrier properties as can be confirmed from the I_{corr} of both the samples after 1 day of exposure. The EE-PMHS-PU 25 wt % coating has I_{corr} in value two orders of magnitude less than the EE-PU 25 wt % (Figure 8).

CONCLUSION

The physical and mechanical properties of EE resins are improved by incorporating aromatic PU. The broad tan δ peak for the hybrid system confirms heterogeneity in the local segmental motion which also contributes to the impact energy absorption for a wide range of temperature. The corrosion inhibition properties of EE and PU hybrid coatings are improved by the addition of PMHS. Analysis of thermomechanical properties confirms the coupling of EE and PU by PMHS.

ACKNOWLEDGMENT

The financial support provided by the office of Naval Research to JSU-UC-ONR project, ONR, N00014-09-1-0980 is gratefully acknowledged.

REFERENCES

1. Ngai, K. L.; Roland, C. M. *Macromolecules* **1993,** *26*, 6824.
2. Lodge, T. P.; McLeish, T. C. B. *Macromolecules* **2000,** *33*, 5278.
3. Roland, C. M.; Casalini, R. *Macromolecules* **2007,** *40*, 3631.
4. Ngai, K. L.; Roland, C. M. *Macromolecules* **1993,** *26*, 2688.
5. Fried, J. R.; Karasz, F. E.; MacKnight, W. J. *Macromolecules* **1978,** *11*, 150.
6. Nyamweya, N.; Hoag, S. W. *Pharm. Res.* **2000,** *17*, 625.
7. Roland, C. M.; Casalini, R. *Macromolecules* **2005,** *38*, 8729.
8. Stannarius, R.; Crawford, G. P.; Chien, L. C.; Doane, J. W. *J. Appl. Phys.* **1991,** *70*, 135.
9. Riccardi, C. C.; Borrajo, J.; Williams, R. J. *J. Macromolecules* **1998,** *31*, 1124.
10. Mucha, M. *Prog. Polym. Sci.* **2003,** *28*, 837.
11. Mobley, R. K. Plant Engineers Handbook. Massachusetts, USA: Butterworth-Heinemann, **2001**, p 12/150.
12. Malshe, V. C.; Waghoo, G. *Prog. Org. Coat.* **2006,** *56*, 131.
13. Lee, J. H.; Lee, J. W. *Polym. Eng. Sci.* **1994,** *34*, 742.
14. Shikha, D.; Kamani, P. K.; Shukla, M. C. *Prog. Org. Coat.* **2003,** *47*, 87.
15. Ramesh, D.; Vasudevan, T. *Prog. Org. Coat.* **2009,** *66*, 93.
16. Marshall, G. L.; Lander, J. A. *Eur. Polym. J.* **1985,** *21*, 959.
17. Moizebelt, W. J.; Nielen, M. W. F. J. *Mass Spectrom.* **1996,** *31*, 545.
18. Meneghetti, S. M. P.; DeSouza, R. F.; Monteiro, A. L.; DeSouza, M. O. *Prog. Org. Coat.* **1998,** *33*, 219.
19. USACE, Manual, EM 1110-2-3400, Painting: New Construction and Maintenance, **1995;** Chapter 4.
20. Ostberg, G.; Hulden, M.; Bergenstahl, B.; Holmberg, K. *Prog. Org. Coat.* **1994,** *24*, 281.
21. Niu, B. J.; Urban, M. W. *J. Appl. Polym. Sci.* **1998,** *70*, 1321.
22. Steward, P. A.; Hearn, J.; Wilkinson, M. C. *Adv. Colloid Interface Sci.* **2000,** *86*, 195.
23. Waters, W. A. *J. Am. Oil. Chem. Soc.* **1971,** *48*, 427.
24. Muizebelt, W. J.; Hubert, J. C.; Venderbosch, R. A. *M. Prog. Org. Coat.* **1994,** *24*, 263.
25. Gorkum, R. V.; Bouwman, E. *Coord. Chem. Rev.* **2005,** *249*, 1709.
26. Ioakimoglou, E.; Boyatzis, S.; Argitis, P.; Fostiridou, A.; Papapanagiotou, K.; Yannovits, N. *Chem. Mater.* **1999,** *11*, 2013.
27. Micciche, F.; Havreren, J. V.; Oostveen, E.; Ming, W.; Linde, R. V. *D. Appl. Catal. A* **2006,** *297*, 1174.
28. Russel, G. A. *J. Am. Chem. Soc.* **1957,** *79*, 3871.
29. Carlsson, D. J.; Ingold, K. U. *J. Am. Chem. Soc.* **1968,** *90*, 1056.
30. Lykakis, I. N.; Vougioukalakis, G. C.; Orfanopoulos, M. J. *Org. Chem.* **2006,** *71*, 8740.
31. Muller, B.; Fischer, S. *Corros. Sci.* **2006,** *48*, 2406.
32. Malshe, V. C.; Waghoo, G. *Prog. Org. Coat.* **2004,** *51*, 172.
33. Muller, B.; Schubert, M. *Eur. Coat. J.* **1999,** *11*, 34.
34. Muller, B.; Oughourlian, C.; Triantafillidis, D. J. *Coat. Technol.* **2001,** *73*, 81.
35. Singh-Beemat, J.; Iroh, J. O. *Prog. Org. Coat.* **2012,** *74*, 173.
36. Tekalur, S. A.; Shukla, A.; Shivakumar, K. *Compos. Struct.* **2008,** *84*, 271.
37. Roland, C. M.; Casalini, R. *Polymer* **2007,** *48*, 5747.
38. Hu, H.; Sirong, Y.; Wang, M.; Ma, J.; Liu, K. *Polym. Adv. Technol.* **2009,** *20*, 748.
39. Bogoslovov, R. B.; Roland, C. M. *Appl. Phys. Lett.* **2007,** *90*, 2219101.
40. Lawrence, N. J.; Bushell, S. M. *Tetrahedron Lett.* **2000,** *41*, 4507.
41. Mimoun, H. J. *Org. Chem.* **1999,** *64*, 2582.

42. Lawrence, N. J.; Drew, M. D.; Bushell, S. M. *J. Chem. Soc. Perkin Trans.* **1999,** *1*, 3381.
43. Kobayashi, Y.; Takahisa, E.; Nakano, M.; Watatani, K. *Tetrahedron* **1997,** *53*, 1627.
44. Nelson, T. MS Thesis, University of Cincinnati, Ohio, **2006.**
45. Tuttle, T.; Wang, D.; Thiel, W.; Kohler, J.; Hofman, M.; Weis, J. J. *Organomet. Chem.* **2007,** *692*, 2282.
46. Patai, S.; Rappoport, Z. The Chemistry of Organic Silicon Compounds; Wiley: New York, **1989.**
47. McCrum, N. G.; Buckley, C. P.; Bucknail, C. B. Principles of Polymer Engineering; Oxford: New York, **1988.**
48. Wada, Y.; Kasahara, T. J. *Appl. Polym. Sci.* **1967,** *11*, 1661.
49. Lotti, C.; Correa, C. A.; Canevarolo, S. V. *Mater. Res.* **2000,** *3*, 37.